

## CPW and Microstrip Line-Fed Compact Fractal Antenna for UWB-RFID Applications

Hafid Tizyi<sup>1, \*</sup>, Fatima Riouch<sup>1</sup>, Abdelwahed Tribak<sup>1</sup>,  
Abdellah Najid<sup>1</sup>, and Angel Mediavilla<sup>2</sup>

**Abstract**—In this study, we present an implementation of Ultra Wide Band (UWB) Koch Snowflake antenna for Radio Frequency Identification (RFID) applications. The compact antenna, based on the Koch Snowflake shape, is fed by coplanar waveguide (CPW) and by microstrip line with an overall size of  $31 \times 27 \times 1.6 \text{ mm}^3$ . The simulation analysis is performed by CST Microwave Studio and compared with HFSS software. The antenna design exhibits a very wide operating bandwidth of 13 GHz (3.4–16.4 GHz) and 11 GHz (3.5–14.577 GHz) with return loss better than 10 dB for microstrip line antenna and CPW antenna respectively. A prototype of CPW and microstrip antenna was fabricated on an FR4 substrate and measured. Simulated and measured results are in close agreement. The small size of the antenna and the obtained results show that the proposed antenna is an excellent candidate for UWB-RFID localization system applications.

### 1. INTRODUCTION

Radio Frequency Identification is one of the fastest growing wireless technologies in recent years. A basic RFID system consists of two components, a reader and a transponder (tag). The reader sends an RF signal to scan all available tags, and the tags receive the RF signal and reply the backscattered signal to the reader [1].

RFID became a universal technology, and its application has been found in more advanced applications such as distribution, logistics, homeland and personal security, distributed sensor networks, and bioengineering [2].

However, the conventional RFID systems based on narrowband present various problems which limit the use of the RFID techniques in universal wireless sensing and localization systems, such as relatively short operating range (4–5 m), low positional accuracy, low throughput, and low immunity to signal degradation and multipath effects [3]. To solve these problems in RFID systems, increasing interest is paid to apply UWB technology for RFID.

The UWB technology is one of the most promising solutions for future wireless and RFID applications due to its advantages such as low consumption, high data rate, excellent immunity to multipath propagation and a high degree of reliability. Another important advantage is that using the wideband frequency spectrum containing high frequencies used for more localization of the microwave energy at a specific target and low frequencies enables the microwave signal to penetrate through some obstacles deeply [4].

Since the Federal Communications Commission (FCC) allowed [3.1–10.6] GHz unlicensed band for UWB applications, this technology has become very popular and found widespread applications in

---

*April 11 January 2016, Accepted 30 June 2016, Scheduled 11 July 2016*

\* Corresponding author: Hafid Tizyi (tizyi@inpt.ac.ma).

<sup>1</sup> STRS Lab., National Institute of Posts and Telecommunications INPT, Rabat, Morocco. <sup>2</sup> DICOM University of Cantabria, Santander, Spain.

communication systems [5], land-mine detection [6], radar systems [7], and biomedical applications, such as breast cancer detection [8].

In UWB-RFID systems, the design of an antenna is one of the most challenging problems to be solved, because UWB systems need the antenna with a sufficiently broad operating bandwidth for impedance matching and high-gain radiation in limited volume and compact size. Recently, several publications have been published on the appealing UWB into RFID localization and tracking systems [4–9]. This technique has been firstly investigated in RFID application for UHF/VHF bands. The history and the state of the art in UWB antennas were presented in [9].

Fractal antennas are preferred in UWB-RFID technology due to their numerous advantages, such as small size, light weight, and easy installation, in addition to their extremely wide band [10–12].

This research aims to develop a UWB Koch snowflake antenna applied to RFID location systems. The antenna is designed as the radiating element of a miniaturized UWB RFID transmitter. The microstrip antenna is created by introducing techniques that improve the bandwidth. There are two methods to increase the bandwidth of a patch antenna [22].

The first involves coupling several resonances. Equation (1) shows that when ‘ $h$ ’ increases, the bandwidth also increases.

$$\begin{cases} \text{BW} = 3.77 \cdot \frac{\epsilon_r - 1}{(\epsilon_r)^2} \frac{L \cdot h}{\lambda \cdot w} & \text{for } h \ll \lambda \\ \text{BW} = 3.77 \cdot \frac{\epsilon_r - 1}{(\epsilon_r)^2} \frac{h}{\lambda} & \text{for } W \ll L \end{cases} \quad (1)$$

where  $\lambda$ ,  $h$ ,  $W$ ,  $L$ ,  $\epsilon_r$  are the wavelength, height, width, length and relative permittivity of the substrate, respectively.

The second method used in this paper is to reduce the quality factor ( $Q$ ) of a resonance (Equation (2)). To do so, we can add an inductive element (stubs), a capacitive element (slots) or both. Also, it can be achieved by adding a lossy element or by a progressive evolution of the impedance between the feedline and the radiating element:

$$\text{BW} = \frac{f_{res}}{Q} \quad (2)$$

With  $f_{res}$  resonant frequency.

## 2. ANTENNA DESIGN

The Snowflake-Koch is a fractal shape constructed by starting with an equilateral triangle (zero iteration) (Fig. 1(a)). The first iteration is composed of two united solid equilateral triangles in the

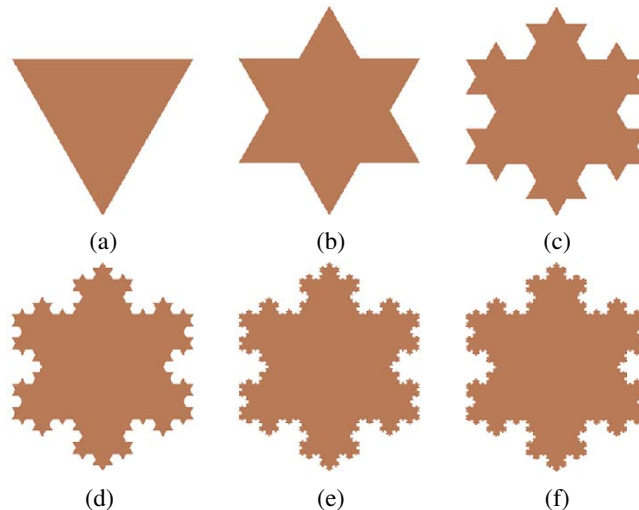


**Figure 1.** The Koch Snowflake antenna.

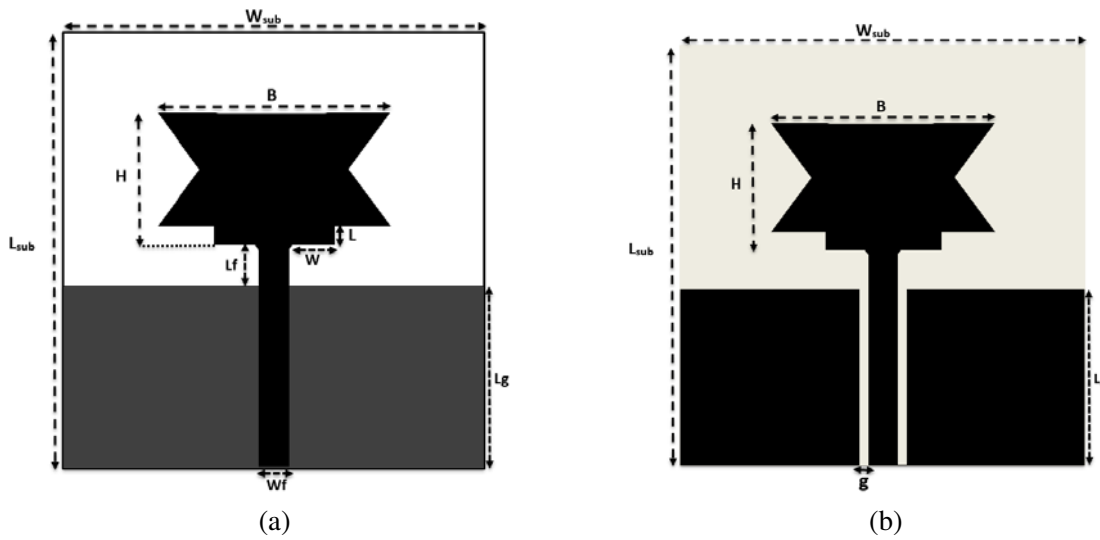


**Figure 2.** The geometry of the proposed antenna: (a) microstrip fed antenna, (b) CPW fed antenna.

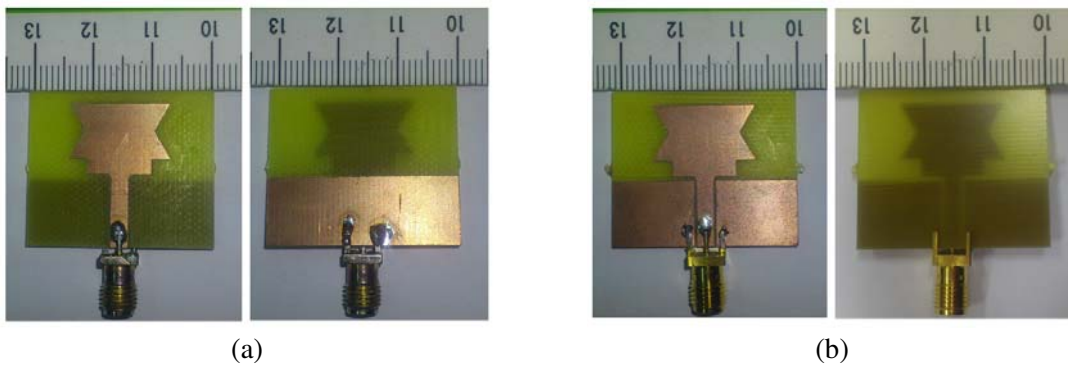


**Figure 3.** Fabricated antenna fed by: (a) microstrip line and (b) CPW.

same plane as illustrated in Fig. 1(b). For the higher iterations, the Koch antenna is constructed by adding smaller and smaller triangles to the structure as shown in Fig. 1.

The geometries of the UWB fractal antenna fed by microstrip line and CPW are depicted in Figs. 2(a) and (b), respectively. It is based on the first iteration Koch Snowflake (Fig. 1(b)). The antenna is printed on a dielectric substrate FR4 (Fig. 3) with a thickness of 1.6 mm,  $\tan \delta$  of 0.024, and relative permittivity of  $\epsilon_r = 4.4$ . The substrate dimensions are  $31 \times 27 \text{ mm}^2$ , and the feedline has a width  $W_f = 3 \text{ mm}$ . This corresponds to a characteristic impedance of  $50 \Omega$ .

Figure 4 depicts the steps used to develop the antenna, by introducing techniques that broaden the bandwidth mentioned in the first section, namely:

- Step 1.** Create a Fractal Koch Snowflake antenna (first iteration) fed by a microstrip line with a total ground plane (Ant. 1). The design procedure of the original Koch antenna is provided in [21].
- Step 2.** Use a partial ground plane for increasing the bandwidth (Ant. 2).
- Step 3.** Add a rectangular element between the feedline and radiation element in order to have a progressive evolution of the impedance between the feedline and radiating element) (Ant. 3).
- Step 4.** Remove the top triangle of the fractal antenna for good impedance matching between the feed line and radiating element (Ant. 4).

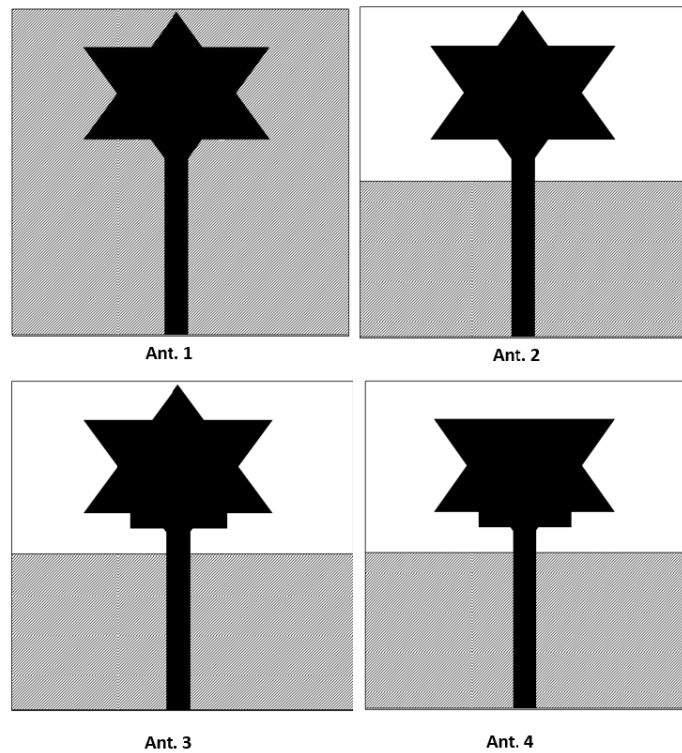
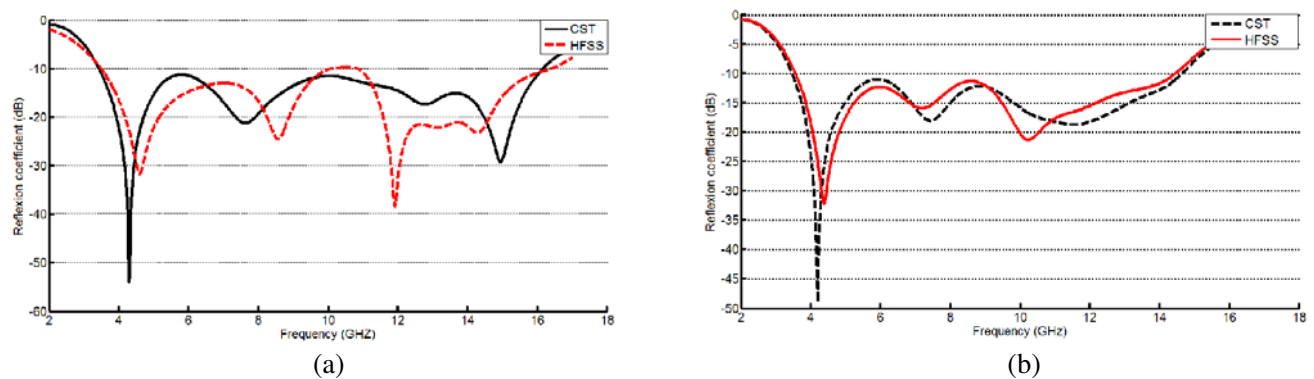


**Figure 4.** Different steps followed in the implementation of the proposed antenna.

### 3. SIMULATION AND MEASUREMENT RESULTS

The simulation of the Koch fractal antenna is performed using the time domain analysis tools from Computer Simulation Technology (CST) Microwave Studio. This provides a wide range of time domain signal that is used in UWB system. The numerical analysis of the software tools is based on the Finite Integration Technique (FIT) [15]. For comparison purpose, High-Frequency Structural Simulator (HFSS) in the frequency domain, based on the Finite Element Method (FEM) [16], is performed.

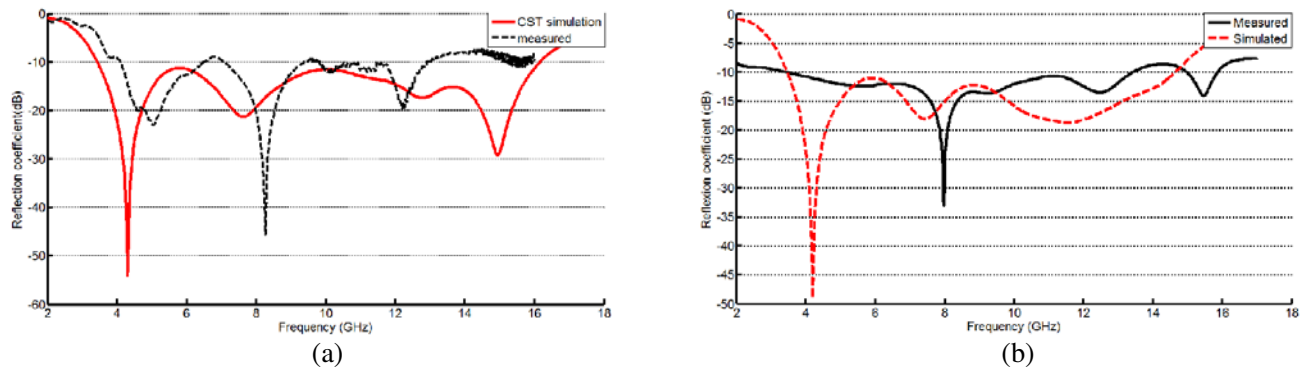
After all the design steps and optimization, the proposed antenna is fabricated using LPKF ProtoMat S63. A prototype was milled on an FR4 epoxy substrate; an SMA coaxial connector was attached to the feedline end, as seen in Fig. 3. Then, it is measured experimentally using the Anritsu Vector Network Analyzer.



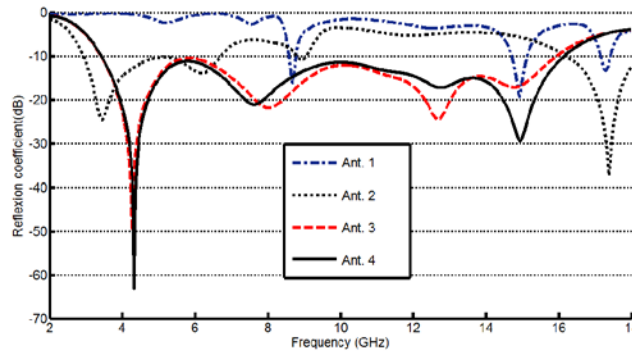
**Figure 5.** Simulated reflection coefficient for: (a) microstrip antenna, (b) CPW antenna.

**Table 1.** Optimized antenna parameters.

Dimensions	$W_{\text{sub}}$	$L_{\text{sub}}$	$L_f$	$W_f$	$L$
Value (mm)	31	27	0.8	3	2.7
Dimensions	$L_g$	$g$	$H$	$B$	$W$
Value (mm)	11	0.35	1	18	3.59



**Figure 6.** Simulated and measured results of: (a) microstrip antenna, (b) CPW antenna.



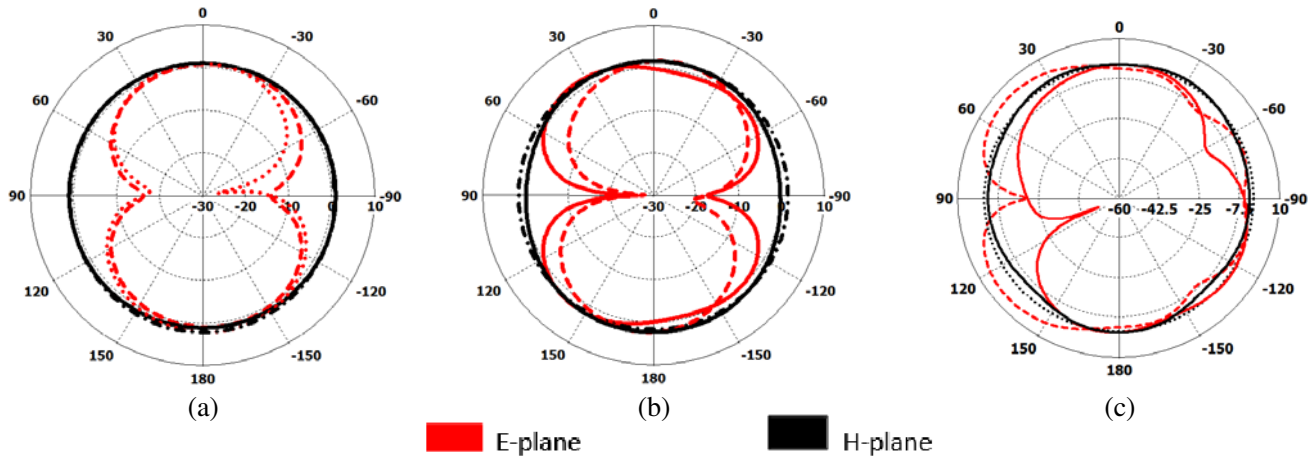
**Figure 7.** Simulated reflection coefficient for Ant. 1, Ant. 2, Ant. 3, and Ant. 4 (Fig. 2).

Figure 5 illustrates the simulated results obtained by both simulation tools of the return loss of the proposed antenna with the optimized parameters as listed in Table 1. The figure shows that the antenna has a wide and excellent impedance matching bandwidth (with VSWR less than 2) across the UWB band with return loss, less than 10 dB in the band 3.4–16.4 GHz. We can also note a good agreement between simulated results.

Figure 6 shows the comparison between measured and simulated results of the proposed antenna. We can see that there is a close agreement between the measured and simulated results. We can also observe some disagreements between simulation and measurement results in this figure. This is due to uncertainly in substrate dielectric constant and in some practical limitation such as SMA connector quality, bad soldering effect and fabrication tolerance.

A parametric study, which was done to show the effects of return loss for a different element or steps (Fig. 4) of the antenna, is presented in Fig. 7. As shown in this figure, the use of partial ground plane technic and the addition of a rectangular element between radiation element and feed line allows improving adaptation of the impedance.

Antenna radiation pattern gives the radiation properties on an antenna as a function of space coordinates. For the linearly polarized antenna, performance is often described in terms of the  $E$ -plane ( $XY$ -plane) and  $H$ -plane ( $YZ$ -plane) patterns [13]. Fig. 8 and Fig. 9 show the radiation patterns at



**Figure 8.** The radiation patterns of the microstrip fed antenna in the  $E$ -plane and  $H$ -plane at (a) 3.6 GHz, (b) 5.8 GHz, (c) 10 GHz.

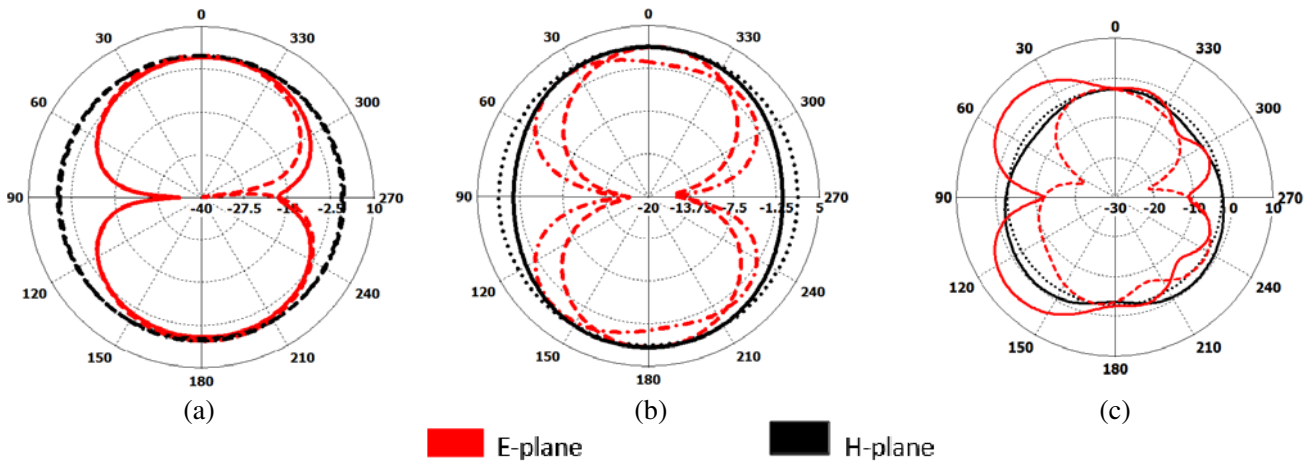


**Figure 9.** The radiation patterns of the CPW fed antenna in the  $E$ -plane and  $H$ -plane at (a) 3.6 GHz, (b) 5.8 GHz, (c) 10 GHz.

3.6 GHz, 5.8 GHz and 10 GHz of the microstrip-fed antenna and CPW-fed antenna in the  $E$ -plane and  $H$ -plane. We can see that the antenna has good omnidirectional radiation patterns at lower frequencies in the  $E$  and  $H$ -planes, and nearly directive in the  $E$ -plane at high frequencies. This pattern is suitable for our applications and in most wireless communication equipment.

Figures 10 and 11 show the cross-polar of the proposed antenna. This parameter presents the polarization orthogonal to a reference polarization. The cross-polar less than  $-19$  dB at low frequency (3.6 GHz and 5.8 GHz) and less than  $-12$  dB at high frequency has been achieved. We can see that the microstrip antenna and CPW antenna have the same level of cross-polar.

The group delay of the proposed antenna is shown in Fig. 12. Group delay is an important parameter in the design of the UWB antenna since it gives the distortion of the transmitted pulses in the UWB communications. For good pulse transmission, the group delay should be nearly constant in the overall UWB [14].

As can be seen, the variation of the group delays for both antennas are approximately constant for the entire UWB, except for a sharp change in the lower band at 4.3 GHz. This confirms that the proposed UWB antenna is suitable for UWB communications. The figure also shows that the CPW antenna group delay is more constant than the microstrip antenna group delay.

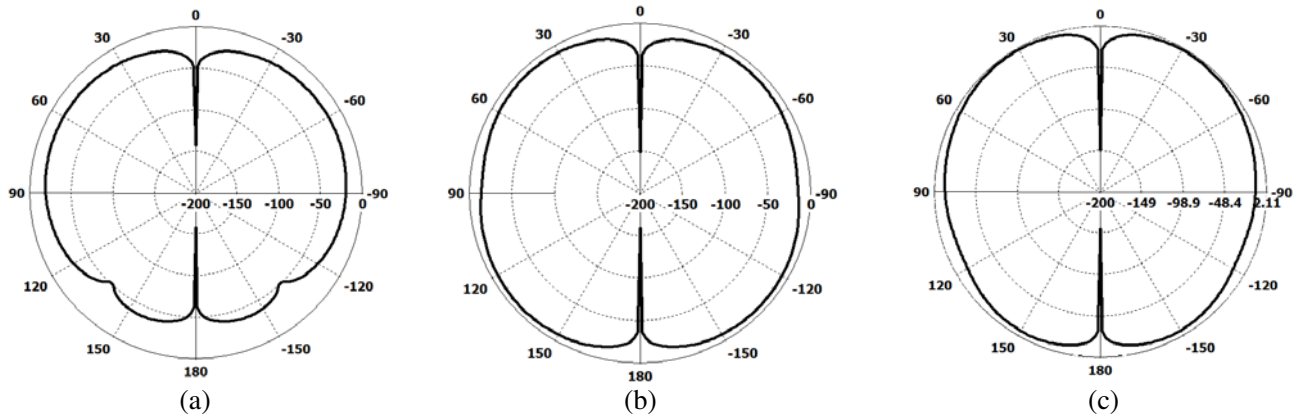


Figure 10. The cross-polar of the microstrip fed antenna at (a) 3.6 GHz, (b) 5.8 GHz, (c) 10 GHz.

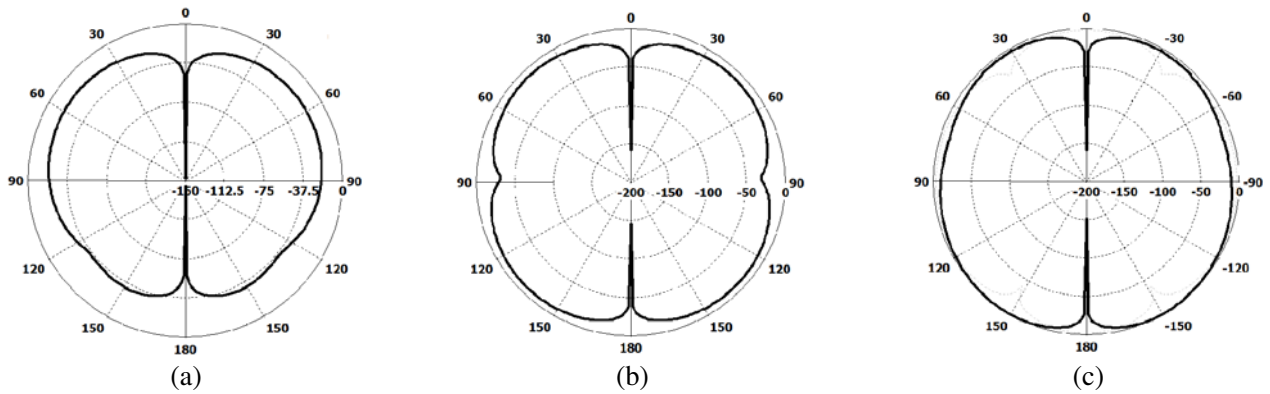


Figure 11. The cross-polar of the CPW fed antenna at (a) 3.6 GHz, (b) 5.8 GHz, (c) 10 GHz.

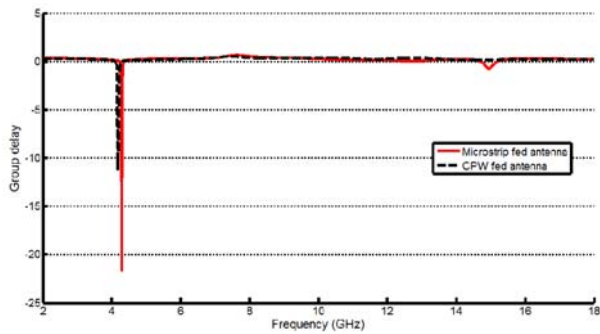


Figure 12. Group delay vs frequency of the proposed antenna.

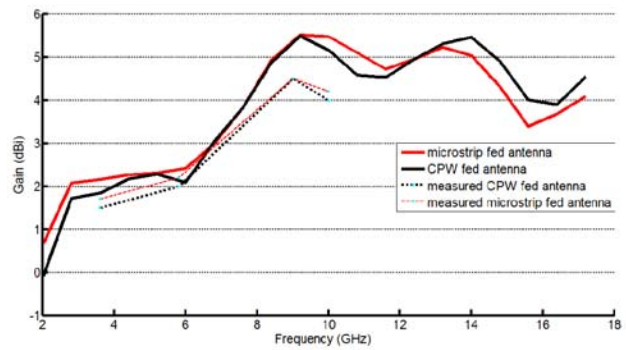


Figure 13. Gain vs frequency of the proposed antenna.

A gain of more than 2 dBi over the whole frequency band is obtained (Fig. 13). The value of the gain is greater than 5 dBi in the frequency ranges of 8 GHz–11 GHz and 12.5 GHz–14 GHz which is sufficient for the use in UWB-RFID application and in most UWB applications such as in Ground Penetrating Radars (GPR) and Breast Cancer detection [7, 8]. We can also observe in this figure that the microstrip antenna presents higher gain in the low and middle frequency, compared to the CPW antenna, and vice versa.

To demonstrate the added value of the proposed design to the previously published results, the

**Table 2.** Performance comparison of this proposed antenna with the previous ones.

	Bandwidth (GHz)	Gain (dBi)	Dimension (mm <sup>2</sup> )	Substrate	Antenna type
Our wok with microstrip antenna	3.4–16.4	between 2.14–5.75	27 × 31	FR4 $\epsilon_r = 4.4$	Modified Koch Snowflake
Our wok with CPW antenna	3.4–14.6	between 1.74–5.75	27 × 31	FR4 $\epsilon_r = 4.4$	Modified Koch Snowflake
Ref. [4]	1–5	< 4.55	82 × 92	Teflon $\epsilon_r = 4.3$	Vivaldi
Ref. [5]	3–12	< 2	50 × 47.5	RT/Duriod $\epsilon_r = 3$	Inverted cone PICA
Ref. [17]	2.78–9.78	—	42 × 50	FR4 $\epsilon_r = 4.7$	Circular disc monopole
Ref. [18]	Three UWB bands between 2–11	Between –4.5–5.5	50 × 50	FR4 $\epsilon_r = 4.4$	Fractal koch and T-shape
Ref. [19]	Two bands Between 2.1–11.8	—	50 × 44	FR4 $\epsilon_r = 4.4$	Modified circular disc with cross-shaped slot
Ref. [20]	2.3–13.2	< 1.86	46 × 52	FR4 $\epsilon_r = 4.4$	Circular disc

following table sums up the advantages of the proposed antenna comparing to the other antenna proposed in the literature. It can be seen that the proposed antenna is miniaturized and presents a wider matching impedance bandwidth and higher gain.

#### 4. CONCLUSION

In this paper, a simple and compact UWB antenna fed by microstrip line and CPW, based on the modifications made to the original Koch fractal antenna to achieve enhanced performance for UWB-RFID applications is presented. The antenna was simulated using CST and HFSS software, realized on an FR4 substrate and tested by Anritsu VNA. The antenna operates at 3.4–16.4 GHz and presents a significant gain higher than 5 dB, an excellent impedance matching (VSWR less than 2) in the total band and an omnidirectional radiation pattern. By transforming the microstrip line feed to CPW, the gain and radiation characteristics are conserved, but the bandwidth decreases with 2 GHz. The comparison between simulated and experimental results shows a good agreement. The antenna is also compared to other related works, and the results show that the proposed antenna presents the widest matching impedance bandwidth, small size, and high gain. These results indicate that the developed antenna is a suitable candidate which can be used to develop an antenna array of smart UWB-RFID systems as well as for other UWB applications that require small size, low cost and important bandwidth, such as microwave radiometry.

#### REFERENCES

1. Tizyi, H., F. Riouch, A. Najid, A. Tribak, and A. S. Mediavilla, “Design of a compact dual-band microstrip RFID reader antenna,” *International Journal of Microwave and Optical Technology*, Vol. 11, No. 2, 137–144, Mar. 2016.
2. Finkensteller, K., *RFID Handbook*, 2nd Edition, Wiley and Sons, 2003.
3. Toccafondi, A. and C. D. Giovampaola, “Design and analysis of a compact antenna for UWB RFID applications,” *2012 IEEE Antennas and Propagation Society International Symposium (APSURSI)*, 1–2, Jul. 8–14, 2012.



4. Aldhaeabi, M., K. Jamil, and A. R. Sebak, "Ultra-wideband antenna for RFID underground oil industry application," *2014 2nd International Conference Artificial Intelligence, Modelling and Simulation (AIMS)*, 333–338, Nov. 18–20, 2014.
5. Alomainy, A., A. Sani, J. Rahman, G. Santas, and Y. Hao, "Transient characteristics of wearable antennas and radio propagation channels for ultra wideband body-centric wireless communications," *IEEE Transactions on Antennas and Propagation*, 875–884, 2009.
6. Hayashi, M. and N. Sato, "A fundamental study of bistatic UWB radar for detection of buried objects," *Proceeding of the 2008 IEEE International Conference on Ultra-Wideband*, 125–128, 2008.
7. Daniels, J. D., *Surface-penetrating Radar (IEE Radar, Sonar Navigation Avionics Series, 6)*, 72–93, IEEE Press, New York, 1996.
8. Teo, J., Y. Chen, and C. Soh, "An overview of radar based ultra wideband breast cancer detection algorithms," *International Journal of Ultra Wideband Communications and Systems*, Vol. 1, 273–281, 2010.
9. Solis, M. A. P., G. M. G. Tejada, and H. J. Aguilar, "State of the art in ultra-wideband antennas," *2005 2nd International Conference Electrical and Electronics Engineering*, 101–105, Sep. 7–9, 2005.
10. Jahroni, M. N. and A. Falahati, "Classic miniature fractal monopole antenna for UWB applications," *Proceeding of ICTTA*, Damascus, Syria, 2008.
11. Jahromi, M. N. and N. Komjani, "Analysis of a modified Sierpinski Gasket monopole antenna printed on dual band wireless devices," *IEEE Transaction on Antennas and Propagation*, Vol. 52, 2571–2579, 2004.
12. Song, C. T. P., P. S. Hall, H. G. Shiraz, and D. Wake, "Fractal stacked monopole with very wide bandwidth," *Electron. Lett.*, Vol. 35, 945–946, 1999.
13. Lim, K.-S., M. Nagalingam, and C.-P. Tan, "Design and construction of microstrip UWB antenna with time domain analysis," *Progress In Electromagnetic Research M*, Vol. 3, 153–164, 2008.
14. Gautam, A. K., Y. Swati, and K. Binod, "A CPW-fed compact UWB microstrip antenna," *IEEE Antennas and Wireless Propagation Letters*, Vol. 12, 151–154, 2013.
15. CST Tool, available on <https://www.cst.com>.
16. HFSS Tool, available on <http://ansoft-hfss.software.informer.com/13.0/>.
17. Liang, J., C. C. Chiau, X. Chen, and C. G. Parini, "Printed circular disc monopole antenna for ultra-wideband applications," *Electron. Lett.*, Vol. 40, No. 20, 1246–1247, Sep. 30, 2004.
18. Zarrabi, F. B., Z. Mansouri, N. P. Gandji, and H. Kuhestani, "Triple notch UWB monopole antenna with fractal Koch and T-shape stub," *AEUE — International Journal of Electronics and Communications*, Vol. 70, No. 1, 64–69, 2015.
19. Sasibhushana Rao, G., K. Srinivasa Kumar, and R. Pillalamarri, "Cross-shaped slot printed UWB monopole antenna with notch function," *Microsystem Technologies*, Vol. 21, No. 11, 2327–2330, 2015.
20. Sasibhushana Rao, G., K. Srinivasa Kumar, and R. Pillalamarri, "Printed planar circular radiating patch ultra wideband antennas," *Microsystem Technologies*, Vol. 21, No. 11, 2321–2325, 2015.
21. Borja, C. and J. Romeu, "On the behavior of Koch island fractal boundary microstrip patch antenna," *IEEE Transactions on Antennas and Propagation*, Vol. 51, No. 6, 1281–1291, Jun. 2003.
22. Hoole, P. R. P., K. Pirapaharan, and S. R. H. Hoole, *Analyse and Design of Electrical and Electronic Device and Systems*, WIT Press, 2013.